Quantum Simulation of False Vacuum Decay on Current Quantum Hardware

James Ingoldby

Durham University, IPPP

QuantHEP, Queen Mary Univerity London,
15th June 2026

Outline

Acknowledgments

Work in preparation with J. Fraxanet, M. Spannowsky, S. Williams, and M. Wingate.

We gratefully acknowledge the NQCC for facilitating access to IBM quantum hardware.

False-Vacuum Decay

Metastable Vacuum Decay

A QFT starts in excited state but quantum tunnels to true ground state (vacuum) - bubbles nucleate.

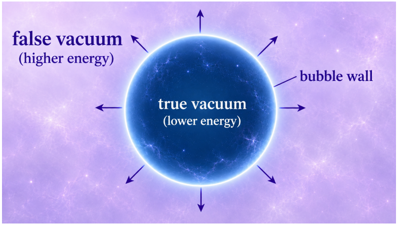

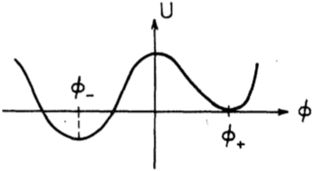

Figure: Field will quantum tunnel from ϕ_+ to ϕ_- [Coleman '77]

- Small bubbles shrink: wall tension dominates
- Critical bubbles expand: volume energy wins
- The decay is classically forbidden

From Cosmology to Condensed Matter

A central process in cosmology and statistical physics

$$V(H) = \lambda(|H|^2 - v^2)^2 \,.$$

Higgs mass measurements imply λ may run negative [Elias-Miró et al '11]

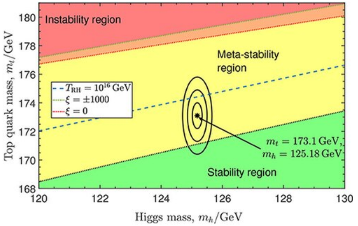

Figure: Recent determination of SM parameters: [Markannen et al '18]]

Provides constraint on BSM

FVD in early universe could provide gravitational wave signatures.

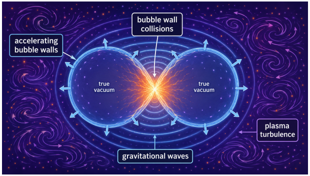

Arises in Ising ferromagnets and supercooled fluids.

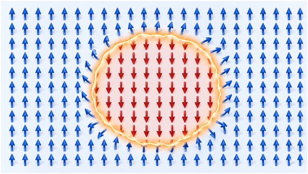

Semiclassical Decay Rate

$$\Gamma = \frac{\mu}{2\pi} \exp\left[-\pi \frac{m^2}{\mu}\right]$$

- m: kink/domain-wall mass
- μ: energy-density splitting between false and true vacua
- In $1+1$d, bubble nucleation creates a kink–antikink pair

[Preskill and Vilenkin '93]

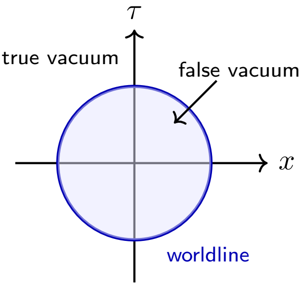

$$S_E(R) = 2\pi R m - \pi R^2 \mu$$

What this does not tell us

- Thin-wall/defect approximation: assumes sharp kink worldlines.
- The "false vacuum" is subtle in full quantum field theory.
- The Euclidean calculation gives a rate, not the real-time bubble growth and collision dynamics.

The O'Brien–Fendley Model

Hamiltonian

$$\mathcal{H}_{\mathrm{OBF}} = -\sum_i Z_i Z_{i+1} - g_x \sum_i X_i + \lambda \sum_i \big(X_i Z_{i+1} Z_{i+2} + Z_i Z_{i+1} X_{i+2} \big)$$

- **Model of $S = 1/2$ spins**
  1-D chain with nearest- and next-to-nearest-neighbour interactions [O'Brien and Fendley '17]. Each spin represented with a single qubit.
- **Controllable laboratory**
  Simple setting for quantum simulation of false-vacuum decay on a digital qubit-based quantum computer.

Phase Diagram

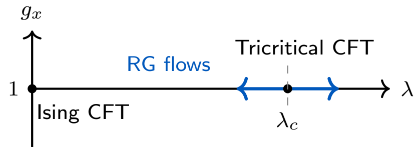

Two Critical Points:

Ising CFT at $g_x = 1$, $\lambda = 0$.

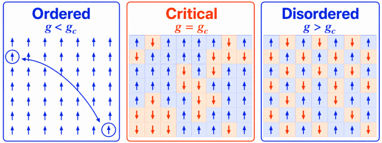

Tricritical Ising CFT at $g_x = 1$, $\lambda = \lambda_c \approx 0.428$.

- KW self-duality preserved along line $g_x = 1$.
- Real time evolution for $\lambda < \lambda_c$ investigated in [Milsted et al '24]
- We focus on region with $g_x = 1$, $\lambda > \lambda_c$.

Continuum QFT

Controlled scaling limits of the qubit-native spin chain exist around the two critical points.

Symmetries

Spin flip: $\eta = \prod_i X_i, \qquad \eta^2 = \mathbb{1}, \qquad \eta^\dagger = \eta.$

Action on other operators $\eta Z_j = -Z_j \eta, \qquad \eta X_j = X_j \eta.$

Symmetries

Spin flip: $\eta = \prod_i X_i, \qquad \eta^2 = \mathbb{1}, \qquad \eta^\dagger = \eta.$
Action on other operators $\eta Z_j = -Z_j \eta, \qquad \eta X_j = X_j \eta.$

KW self-duality: On the periodic chain this *noninvertible* global symmetry is implemented by a nonunitary operator D:

$$\mathsf{D}^\dagger = \mathsf{D}T, \qquad \mathsf{D}^2 = (\mathbb{1} + \eta)\, T^{-1}, \qquad \mathsf{D}\eta = \mathsf{D}\,,$$

for lattice translation T. Explicit construction: [Seiberg, Seifnashri, Shao '24].
Action on other operators $\mathsf{D}X_j = Z_{j-1}Z_j\mathsf{D}, \qquad \mathsf{D}Z_jZ_{j+1} = X_j\mathsf{D}.$

Symmetries

Spin flip: $\eta = \prod_i X_i, \qquad \eta^2 = \mathbb{1}, \qquad \eta^\dagger = \eta.$
Action on other operators $\eta Z_j = -Z_j \eta, \qquad \eta X_j = X_j \eta.$

KW self-duality: On the periodic chain this *noninvertible* global symmetry is implemented by a nonunitary operator D:

$$\mathsf{D}^\dagger = \mathsf{D}T, \qquad \mathsf{D}^2 = (\mathbb{1} + \eta)\, T^{-1}, \qquad \mathsf{D}\eta = \mathsf{D}\,,$$

for lattice translation T. Explicit construction: [Seiberg, Seifnashri, Shao '24].
Action on other operators $\mathsf{D}X_j = Z_{j-1}Z_j\mathsf{D}, \qquad \mathsf{D}Z_jZ_{j+1} = X_j\mathsf{D}.$

Three degenerate ground states:
if $|\mathcal{G}_\uparrow\rangle$ is a ground state with $\langle\mathcal{G}_\uparrow|Z_j|\mathcal{G}_\uparrow\rangle \neq 0, \quad \langle\mathcal{G}_\uparrow|X_j|\mathcal{G}_\uparrow\rangle = 0,$
then $|\mathcal{G}_\downarrow\rangle = \eta|\mathcal{G}_\uparrow\rangle$ and $|\mathcal{G}_0\rangle = \mathsf{D}\frac{1+\eta}{2}|\mathcal{G}_\uparrow\rangle$ also ground states.

Symmetries

Spin flip: $\eta = \prod_i X_i, \qquad \eta^2 = \mathbb{1}, \qquad \eta^\dagger = \eta.$
Action on other operators $\eta Z_j = -Z_j \eta, \qquad \eta X_j = X_j \eta.$

KW self-duality: On the periodic chain this *noninvertible* global symmetry is implemented by a nonunitary operator D:

$$\mathsf{D}^\dagger = \mathsf{D}T, \qquad \mathsf{D}^2 = (\mathbb{1} + \eta)\, T^{-1}, \qquad \mathsf{D}\eta = \mathsf{D}\,,$$

for lattice translation T. Explicit construction: [Seiberg, Seifnashri, Shao '24].
Action on other operators $\mathsf{D}X_j = Z_{j-1}Z_j\mathsf{D}, \qquad \mathsf{D}Z_jZ_{j+1} = X_j\mathsf{D}.$

Three degenerate ground states:
if $|\mathcal{G}_\uparrow\rangle$ is a ground state with $\langle\mathcal{G}_\uparrow|Z_j|\mathcal{G}_\uparrow\rangle \neq 0, \quad \langle\mathcal{G}_\uparrow|X_j|\mathcal{G}_\uparrow\rangle = 0,$
then $|\mathcal{G}_\downarrow\rangle = \eta|\mathcal{G}_\uparrow\rangle$ and $|\mathcal{G}_0\rangle = \mathsf{D}\frac{1+\eta}{2}|\mathcal{G}_\uparrow\rangle$ also ground states.
Take the spin-flip even combination $|\mathcal{G}_+\rangle = (|\mathcal{G}_\uparrow\rangle + |\mathcal{G}_\downarrow\rangle)/\sqrt{2}$.

$$\langle\mathcal{G}_0|X_j|\mathcal{G}_0\rangle = \langle\mathcal{G}_+|Z_jZ_{j+1}|\mathcal{G}_+\rangle.$$

Vacuum Structure

For the special value, $\lambda = 0.5$, the three ground states can be determined exactly on the ring for any $N \geq 3$ spins [O'Brien and Fendley '17]

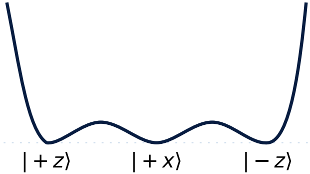

$$|+Z\rangle = |\uparrow \ldots \uparrow\rangle, \quad |+X\rangle = |\updownarrow \ldots \updownarrow\rangle, \quad |-Z\rangle = |\downarrow \ldots \downarrow\rangle\,,$$

where $|\updownarrow\rangle \equiv \frac{|\uparrow\rangle + |\downarrow\rangle}{\sqrt{2}}$. We shall start our spin chain off in the state $|+X\rangle$.

$\lambda = 0.5$ is close to $\lambda_c \approx 0.428 \implies$ approx continuum physics.

Continuum Limit

Scale towards tricritical Ising

Approach the tricritical point $\lambda \to \lambda_{c,+}$. Lattice spacing vanishes:

$$ma \sim |\lambda - \lambda_c|^{1/(2-\Delta_{\epsilon'})}, \qquad \Delta_{\epsilon'} = \frac{6}{5}.$$

Continuum interpretation

Near λ_c, changing λ mainly turns on the relevant TCI operator

$$H = H_{\mathrm{TCI}} + g_H \int dx\, \epsilon'(x) + \cdots .$$

Equivalently,

$$S_E = S_{\mathrm{TCI}} + g_E \int d^2x\, \epsilon'(x) + \cdots .$$

Practical consequence

Moving closer to λ_c gives a finer lattice description of the same continuum process.

But for fixed physical volume,

$$L_{\mathrm{phys}} = Na,$$

smaller a means more sites, hence more qubits.

Theory of Kinks

- The OBF model acquires **supersymmetry** [O'Brien and Fendley '17].
- Becomes known integrable model [Zamolodchikov '89]
- S-matrix exhibits a **non-invertible global symmetry with crossing-symmetry violation** [Copetti, Cordova, Komatsu '24].

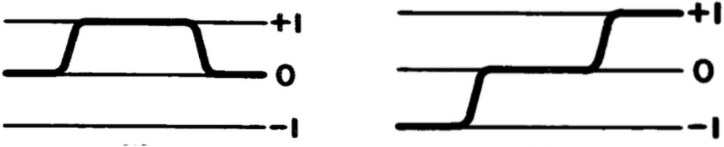

Figure: At low energy, the active degrees of freedom are kinks [Lassig et al '90].

Deforming the Vacuum Structure

Hardware-friendly deformation

Add a local longitudinal field to tilt the vacuum landscape:

$$\mathcal{H} \longrightarrow \mathcal{H}_{\mathrm{OBF}} + g_z \sum_i Z_i$$

This lifts the degeneracy with *minimal circuit overhead*.

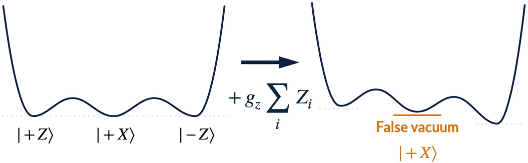

- $|+X\rangle$ becomes the metastable vacuum
- $|+Z\rangle$ becomes the **true vacuum**
- Strength g_z controls the energy gap ε

Real-Time Simulation on Quantum Hardware

State Preparation

Crucial simplification: one Hadamard gate per qubit prepares the metastable vacuum state:

$$H^{\otimes n}|0\rangle^{\otimes n} = |+X\rangle$$

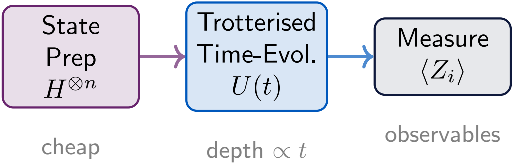

- Trotterisation approximates $U(t) = e^{-i\mathcal{H}t}$; circuit depth grows with t
- The noise budget, not Hilbert-space size, is today's bottleneck

Circuit Decomposition for Time Evolution Operator

Suzuki–Trotter approximation:

$$U(t) = e^{-iHt} \approx \left(\prod_a e^{-i\Delta t H_a} \right)^n .$$

Brick wall circuit layout

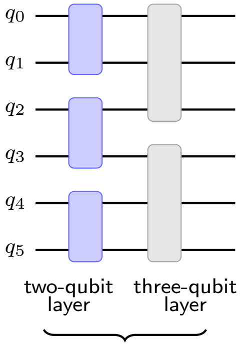

one (schematic) Trotter step

$e^{i\alpha Z_i Z_{i+1}}$

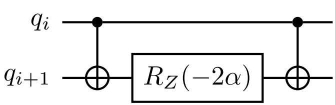

$e^{i\beta Z_i Z_{i+1} X_{i+2}}$

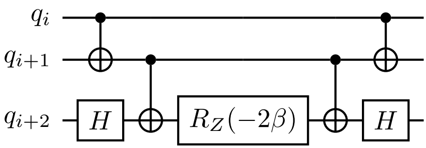

three-qubit block for a ZZX interaction

Classical Benchmark: Tensor Network (TN)

Matrix Product State ansatz

$$|\psi\rangle = \sum_{\{\sigma\}} A^{\sigma_1} A^{\sigma_2} \cdots A^{\sigma_N} |\sigma_1 \cdots \sigma_N\rangle.$$

A^{σ_j} is a $\chi \times d \times \chi$ 3-index tensor. The memory cost scales like

$$O(Nd\chi^2),$$

not $O(d^N)$.

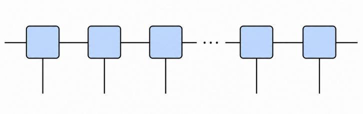

Physical assumption

$$S_{\text{ent}} \lesssim \log \chi.$$

Tensor networks are powerful when the dynamically generated entanglement remains modest.

- Excellent for controlled classical benchmarks
- Systematically improvable by increasing χ
- Not a generic representation of the full Hilbert space

Where Tensor Networks Can Break Down

Bubble dynamics creates entanglement

Nucleation, expansion and collision generate correlations over increasing distances.

Computational consequence

$$\chi_{\text{needed}} \sim e^{S_{\text{ent}}}.$$

If the entanglement grows quickly, classical costs can grow exponentially in time.

Benchmark strategy

Use tensor networks where they converge; use quantum hardware to explore regimes where convergence becomes expensive.

- Larger volumes
- Longer times
- More post-nucleation observables

Classical Simulation of FVD

TN simulation

Evolve the many-body state within a fixed bond-dimension χ Matrix Product State ansatz.

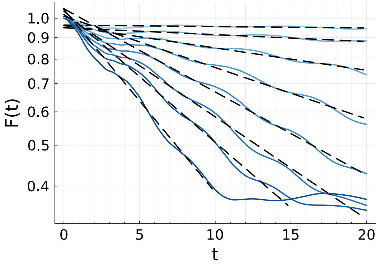

Controlled benchmark window

Increase χ until local observables converge at early and intermediate times.

False-vacuum fraction:

$$F(t) = 1 + \frac{1}{N}\sum_i \langle Z_i \rangle$$

Limitation

Bubble growth/ collision generates entanglement, eventually pushing the required χ beyond what is accessible.

Decays exponentially:

$$F(t) \sim e^{-\gamma t}$$

Decay Rate Extraction

- Exponential suppression at small g_z is the hallmark of *non-perturbative* vacuum decay
- Dependence derived from Coleman's semiclassical calculation in continuum QFT
- Classical tensor networks validate this regime; quantum hardware will push beyond it

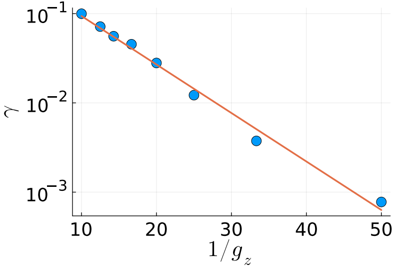

Non-perturbative exponential suppression confirmed

Non-perturbative scaling

$$\log \gamma \sim -\frac{\pi m_c^2}{c} \cdot \frac{1}{g_z}$$

(Preliminary) Results on Quantum Hardware

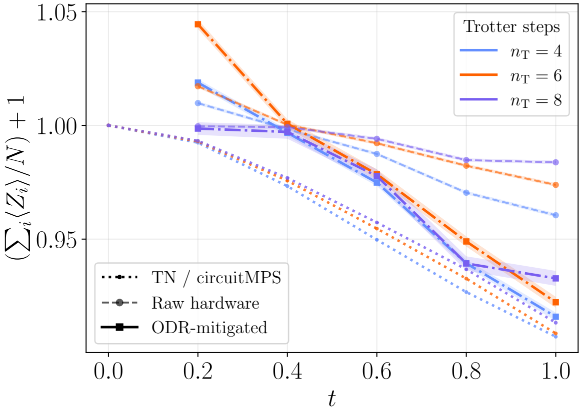

- Result for 80 spins/qubits arranged in a ring on `ibm_boston`.
- Hardware noise very visible in raw data. However ODR error mitigation reduces errors significantly.

Operator Decoherence Renormalisation

Noise model

$$\langle M(t)\rangle_{\mathrm{hw}} \simeq R_M(t)\,\langle M(t)\rangle_{\mathrm{ideal}}$$

$R_M(t)$: operator-dependent renormalisation factor.

ODR correction

$$\langle M(t)\rangle_{\mathrm{ODR}} = \frac{\langle M(t)\rangle_{\mathrm{hw}}}{R_M(t)}$$

Assumption: Noise suppresses observables but doesn't modify the effective Hamiltonian.

Reference circuit

For each Trotter step U, run

$$U_{\mathrm{ref}} = U\,U^{\dagger}.$$

Ideally,

$$U_{\mathrm{ref}}|0\cdots0\rangle = |0\cdots0\rangle.$$

Known answer using same gates

Calibration

$$R_M(t) \simeq \frac{\langle M\rangle^{\mathrm{ref}}_{\mathrm{hw}}}{\langle M\rangle^{\mathrm{ref}}_{\mathrm{ideal}}}$$

Summary and Outlook

What we have shown

False-vacuum decay can be turned into a concrete, qubit-native benchmark for real-time QFT dynamics.

From physics to hardware

- O'Brien–Fendley spin chain: lattice model with a continuum field-theory limit
- TN benchmarks the decay dynamics
- Trotterised evolution implemented on IBM quantum hardware
- Error mitigation crucial

Scope for followup projects

- Push to larger systems, longer times, reduced lattice artefacts
- Diagnose how TN methods begin to fail: entanglement growth, thermalisation, and higher-point observables
- Study kink scattering and how weak breaking of the non-invertible symmetry modifies the S-matrix

Thank you!

James Ingoldby
IPPP, Durham University
james.a.ingoldby@durham.ac.uk

Why Use Quantum Hardware at All?

Exact state-vector memory

A generic n-qubit state requires

$$2^n \text{ complex amplitudes.}$$

For $n = 80$, using 128 bits per complex number,

$$2^{80} \times 16 \text{ bytes} \simeq 1.9 \times 10^{25} \text{ bytes.}$$

Scale comparison

$$1.9 \times 10^{25} \text{ bytes} \simeq 1.9 \times 10^{10} \text{ PB.}$$

Exascale agg. system memory $\sim$O(10) PB.

Even before time evolution, a generic 80-qubit wavefunction is far beyond direct classical storage.

The opportunity

A quantum processor stores the state physically. The challenge is controlling noise and extracting useful observables.

Backup: TDVP

Exact evolution

$$i\partial_t|\psi\rangle = H|\psi\rangle.$$

Projected evolution on MPS manifold

$$|\psi(t)\rangle \in \mathcal{M}_\chi, \qquad i\partial_t|\psi(A)\rangle = P_{T_A\mathcal{M}_\chi} H|\psi(A)\rangle.$$

$$\delta \left\| i\partial_t|\psi(A)\rangle - H|\psi(A)\rangle \right\|^2 = 0.$$

Controlled by

$$\chi, \qquad \Delta t, \qquad \|(1 - P_{T_A\mathcal{M}_\chi})H|\psi(A)\rangle\|.$$